

# Analysis of the Nano Inclusions in a Copper Foil With the Small-Angle X-ray Scattering

Satoshi Yamazaki<sup>\*1</sup>, Yojiro Oba<sup>\*2</sup>, Hirokazu Sasaki<sup>\*1</sup>, Masato Ohnuma<sup>\*3</sup>

**ABSTRACT** The small angle X-ray scattering (SAXS) and the ultra-small angle X-ray scattering (USAXS) measurements were performed for the quantitative evaluation of the nano inclusions and the voids in electrodeposited copper foil. It is presumed that these nano inclusions are the substances added when manufacturing the foil, and that the voids were formed by the aggregation and the disappearance of the nano inclusions at annealing. As a result of the measurements, it was confirmed that there is a clear difference in the scattering intensity between the foil to which an organic additive had been added and the one without an additive in the High- $q$  region where the  $q$  is larger than about  $0.3 \text{ nm}^{-1}$ . In the foil annealed at  $300^\circ\text{C}$ , the scattering intensity increased in the Low- $q$  region. These scattering intensities are presumed to be originated from the nano inclusions and voids, respectively.

## 1. INTRODUCTION

In recent years, the downsizing and the thinning of the mobile devices such as mobile phones and notebook personal computers are advancing, and the downsizing and the thinning are also required for the substrates and the semiconductor packages inside them. Along with this, the micronizing of the internal circuit wiring is also required, and it resulted in the need for a thin and smooth electrodeposited copper foil. In addition, it is also used for the negative electrode current collectors of the lithium ion secondary batteries built in the portable devices stated above, and it is required to reduce its thickness and to increase its strength like the circuit wiring.

Generally, when manufacturing the electrodeposited copper foil, while the electrodepositing solution is passed between a metallic anode and a metallic cathode drum whose surfaces are polished, a direct current is passed between both electrodes to form an electrodeposited copper foil on the surface of the cathode, and the electrodeposited copper foil on the cathode is continuously peeled off (Figure 1). Various additives are added to the copper sulfate bath, and thiourea (TU), which is one of the additives, is used as a brightener for obtaining a gloss. It is known that the TU and the copper form a composite. When the concentration reaches a certain level and exceeds it in a copper sulfate bath, it adsorbs to the growth point of the copper crystal nuclei during film manufacturing, and restrains the crystal growth. For this

reason, countless new nuclei are generated on the plating surface to make the plating film becoming microcrystalline and dense, and it resulted in obtaining a gloss. On the other hand, the decomposition products of the TU form CuS in the electrodeposited copper foil, and are incorporated into the copper foil. These nano inclusions are the cause of the deterioration of the mechanical properties (especially tensile strength and folding endurance) of the electrodeposited copper foil<sup>1)</sup>. Therefore, the method of analyzing them is important in establishing an optimal synthesis condition.

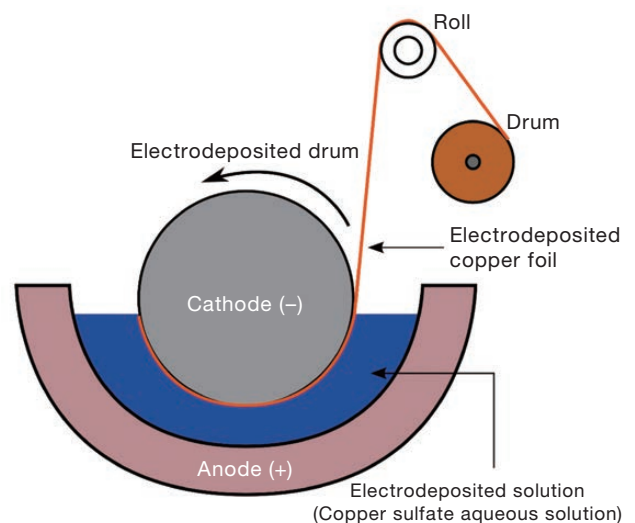


Figure 1 A schematic diagram of a copper foil production.

<sup>\*1</sup> Advanced Technologies R&D Laboratories, R&D Division

<sup>\*2</sup> Japan Atomic Energy Agency

<sup>\*3</sup> Hokkaido University

Same as for the electrodeposited copper foil, the direct observations with a scanning electron microscope (SEM) or a transmission electron microscope (TEM) can be mentioned as a method of evaluating the nano inclusions and the precipitates in the metal. The observation of the nano inclusions in the electrodeposited copper foil has been reported by Y. L. Kao<sup>2)</sup>. However, with respect to the average size and the distribution of the nano inclusions, it is difficult because many observation fields are necessary. On the other hand, the SAXS can obtain the average information about a region which cannot be covered by the TEM or the SEM.

In this paper, we will introduce the outline and the measurement methods related to the SAXS, and we will report the results of the evaluation of inclusions in the electrodeposited copper foil using an synchrotron radiation in practice.

## 2. SAXS

### 2.1 Introduction of the SAXS

The X-ray diffraction (XRD) is the most generally known method as the X-ray scattering in general. In the XRD, when the scattered X-rays in the region of scattering angle:  $2\theta = 5$  to  $90^\circ$  to the incident X-rays are measured, those satisfying the diffraction condition of Bragg are measured as diffraction peaks. The SAXS measures the X-ray scattering with small angles as its name implies, and specifically, when the region is in about  $5^\circ$  or less. This area is called a forgotten area and it is not well known what kind of information is obtained here. However, by analyzing the X-ray scattering in this region, it becomes easier to obtain the average size and the particle size distribution of the inclusions and the precipitates existing in a certain system (metal material, etc.). As Figure 2 shows, as the angle becomes smaller, the average size of the coarser structure can be obtained. In Particular, although the region called the USAXS requires a synchrotron radiation facility which is capable of generating high intensity X-rays, when the USAXS is used, the size of a structure of an utmost maximum of 1000 nm can be evaluated.

To obtain the structural information, electron microscopes such as a TEM, a SEM, or an atomic force microscope (AFM) are also effective means. However, in their measurements, the observation areas are so small that it is difficult to judge whether the observed the nano inclusions or precipitates occupy the majority part or a small part of the whole. On the other hand, the SAXS is an effective measure to follow the structural information of the bulk. Therefore, it can be said that it is in a mutual complementary relationship with the measurement of local structures by electron microscopes, etc. If such structural information and the mechanical properties obtained by a nanoindenter or by a tensile test can be compared, the high strength mechanism can be discussed.

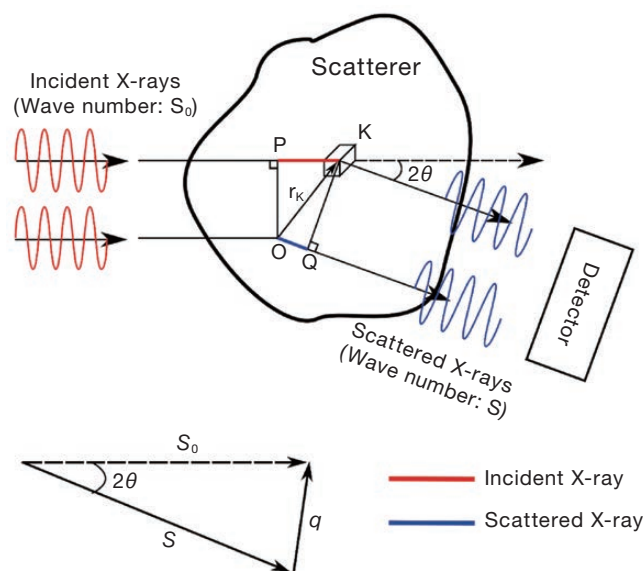


Figure 2 A schematic view the X-ray scattering.

Next, the X-ray scattering of an object will be described in numerical expressions. All the objects are made of atoms, and when X rays are incident on them, the electrons in the atoms are shaken by the X rays and they themselves become the wave sources that generate scattered X-rays. When the scattered X-rays are detected at an angle of  $2\theta$  to the incident X-rays, the superposition of the scattered X-rays generated from every part of the scatterer is detected (Figure 2). There is an optical path difference of the X rays passing through two points, O and K, separated by a distance  $r$ , and the phase difference is given by  $r \cdot q$ . Here, the  $q$  is an amount called a scattering vector, which is defined as a difference of the wave number vectors between the incident X-ray ( $S_0$ ) and the scattered X-ray ( $S$ ), and its absolute value can be expressed as  $|q| = 4\pi \sin \theta / \lambda$  (Figure 2). Therefore, if the electron density distribution of the scatterer is  $\rho(r)$ , the amplitude  $F(q)$  of the scattered X-ray from the sample is given after adding each scattered wave taking the phase difference into consideration:

$$F(q) = \int_V \rho(r) \exp\{-i(q \cdot r)\} dr \quad (1)$$

Since the amount actually detected is not the amplitude but the intensity of the scattered X-ray, the scattering intensity  $I(q)$  is given by:

$$I(q) = |F(q)|^2 \quad (2)$$

Scatterers have various shapes, and the structural factors related to each of them exist. However, since the structures introduced in this paper are all spherical shapes, transforming of the equation (1) using polar coordinates results in:

$$F(q) = 4\pi \int_{r=0}^{\infty} \rho(r) \frac{\sin(qr)}{qr} r^2 dr \quad (3)$$

If the sphere has a radius  $R$  and an electron density of  $\rho$ , it can be derived as:

$$F(q) = V\rho \frac{3\{\sin(qR) - qR \cos(qR)\}}{(qR)^3} \quad (4)$$

The  $V$  here is the volume of the particle. Therefore, the intensity  $I(q)$  can be described as follows.

$$I(q) = V^2 \rho^2 \frac{9}{(qR)^6} [\sin(qR) - (qR) \cos(qR)]^2 \quad (5)$$

In a system to be measured, when the particles are sufficiently dilute, the intensity of the X-ray to be measured is the product of the number of particles in the measured system by the scattering intensities of the individual particles described by the formula (5). Furthermore, taking into account of the size distribution of these particles in the system, the scattering intensity can be described as follows:

$$I(q) = \rho^2 \int_0^{\infty} F^2(q) N(R) dR \quad (6)$$

Here, the  $N(R)$  is the number of particles with radius  $R$ . Therefore, it is possible to obtain the scattering intensity  $I(q)$  of a system with size distribution using various size distribution functions. Incidentally, in this paper, a log-normal distribution is adopted as a size distribution function.

We introduce the information obtained by the SAXS in more detail. The SAXS in Figure 3 is categorized into the following three regions.

Region I (Guinier region):

Size of the particle (average size, rotation radius  $R_g$ )

Region II (the region depending on the particle shape)

Shape of the particle (spherical shape, ellipsoid, column shape, etc.)

Region III (Porod region)

Structure of the particle surface (boundary surface) (smoothness or density profile)

These pieces of information are reflected in the different parts of the scattering curve due to the relative tradeoff between the size of the inclusions or the precipitates and the  $q$  in the measured system. The region I is the smallest angle region, and the boundary with the region II is roughly  $q = 1/R_g$ . This region I is called the Guinier region, and if the particles in the measurement system have uniform electron density, the size can be evaluated from the rotation radius  $R_g$ .

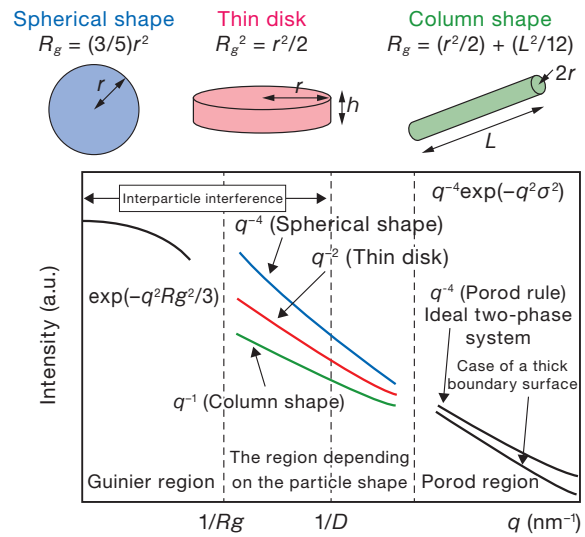


Figure 3 The structural information of the samples obtained by the SAXS.

### 2.2 Use of a Synchrotron Radiation Facility

We will describe the actual optical axis system and the measuring equipment of the SAXS. With respect to the optical axis system of the SAXS, as the Figure 4 shows, incident X-rays are incident on a sample, and then scattered X-rays are detected in a two-dimensional detector installed at the rear of the sample. The SAXS measurements can be categorized into “1: measurement using an laboratory X-ray as a probe” and “2: measurement using a high-luminance synchrotron radiation as a probe”. With respect to the optical axis system, the two measurement methods are in common.

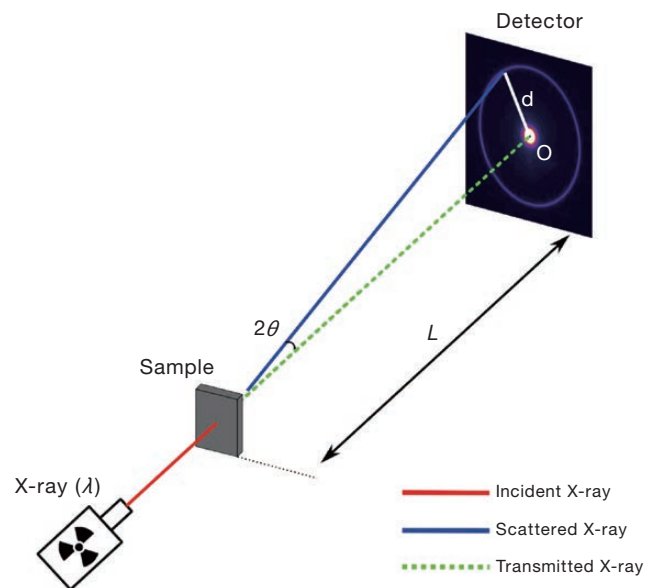


Figure 4 A schematic diagram of the SAXS.

The difference is the distance between the light source and the detector. First, with respect to the light source, since the laboratory X-rays use special X-rays, their wavelengths are uniquely determined by the radiation source, whereas since the high-luminance synchrotron radiation is white light, the wavelength can be selected. With respect to the distance to the detector, it is about 1 m in the laboratory system, whereas in the high-luminance synchrotron radiation, it is possible to separate the sample and the detector by up to 46 m.

As the Figure 4 shows, since the SAXS measures and analyzes the scattered X-rays behind the sample, it is a prerequisite that X-rays pass through the sample. When the sample is composed of relatively light elements such as polymer, it is unnecessary to use the synchrotron radiation with a high luminance. However, when it is composed of elements with a high electron density such as electrodeposited copper foil, it requires high energy X-rays. Specifically, X-rays of 20 keV and above are required, and it is difficult to implement this in laboratory equipment. In addition, an USAXS measurement is possible with the BL19B2 of the SPring-8 which was used this time, and the size evaluation of the structures of sub nm to 1  $\mu\text{m}$  is possible by combining it with the SAXS.

### 3. TEST RESULTS

#### 3.1 Preparation of the Samples

The electrodeposited copper foil added with an organic additive and the one without an additive were prepared, and the foil having a thickness of several tens of  $\mu\text{m}$  was used as measurement samples. The samples were prepared in cooperation with Furukawa Electric's Copper Foil Division. A list of the measured samples is shown in Table 1. In addition, in order to examine the influence of the heat treatment, a part of the electrodeposited copper foil with an organic additive annealed at 300°C in a nitrogen atmosphere was prepared as the Sample 3 (Table 1). For an analysis of the inclusions, a pure copper foil without an additive (Sample 1) was also prepared.

Table 1 The sample list.

Copper foil	Organic additive	Annealing temperature (°C)
Sample 1	Yes	—
Sample 2	No	—
Sample 3	No	300

#### 3.2 Conditions of Each Analysis

The observation was performed using a SEM, and the observation of the voids and the nano inclusions was performed by a TEM. The constituent elements of the nano inclusions were analyzed by the energy dispersive X-ray spectroscopy (EDX).

For the SAXS measurement in the High- $q$  region, the

SAXS equipment installed in the BL19B2 beam line of the SPring-8. And for the USAXS measurement in the Low- $q$  region, the USAXS equipment installed in the same beam line was used. 20 keV was selected as the energy of the incident X-ray, and a two-dimensional position sensitive detector (PILATUS-2M) was used as a detector. The distance between the sample and the detector was 3 m for the SAXS, and 43 m for the USAXS. In order to obtain an absolute value of the scattering intensity, a glassy carbon provided by Mr. Jan Ilavsky of Advanced Photon Source was used as a standard sample for the measurement<sup>3)</sup>. Analysis software Ircan was used for the analysis of the obtained data<sup>4)</sup>.

#### 3.3 Results of the Measurement and the Analysis

According to the previous studies, it has been known that additives are dispersed in copper crystals in the size of several nanometers. STEM observations were performed to confirm whether there were the inclusions in the sizes of several nanometers in our samples. Figure 5 shows the STEM images. As can be seen from the Figure 5 (a), countless dislocations exist in the metallographic structure of the electrodeposited copper foil. Also, from the high-angle annular dark field scanning (HAADF)-STEM image in the Figure 5 (b), it was found that the inclusions of 3 to 5 nm exist in the grain and in the grain boundary of the copper. It can be said that the shape of the inclusions approximates a spherical shape.

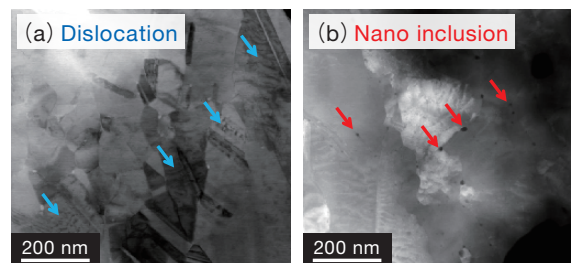


Figure 5 STEM images of the copper foil. (a) Bright-field (BF)-STEM, (b) HAADF-STEM

As a result, an element analysis by the EDX on these inclusions, carbon and sulfur were detected. This is consistent with the results of the previous studies. In the previous studies, the inclusions were concluded to be Cu<sub>2</sub>S, however, from our results, it was newly found that carbon is also included in addition to copper and sulfur.

Next, cross-sectional SEM observation was performed on the electrodeposited copper foil annealed at 300°C (Sample 3). As can be seen from Figure 6, there are multiple voids in the cross section. Since these voids had not existed in the electrodeposited copper foil before annealing (Sample 2), it is considered they were generated by the annealing.



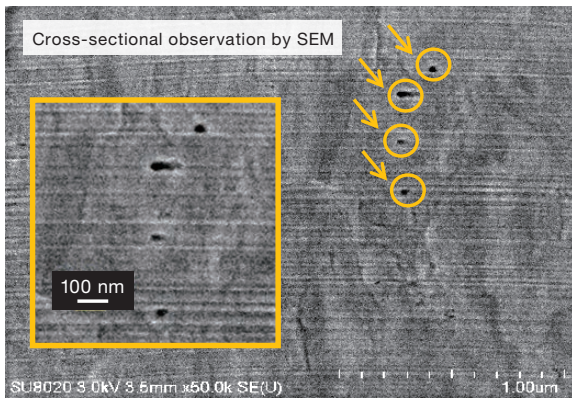


Figure 6 A SEM image of the copper foil

Next shows the results of the USAXS. Figure 7 shows two-dimensional scattering patterns in which the scattering by three sheets of copper foil and oxygen is captured by a two-dimensional detector. It was found that all samples were isotropic and the nano inclusions in the copper foil were isotropically distributed.

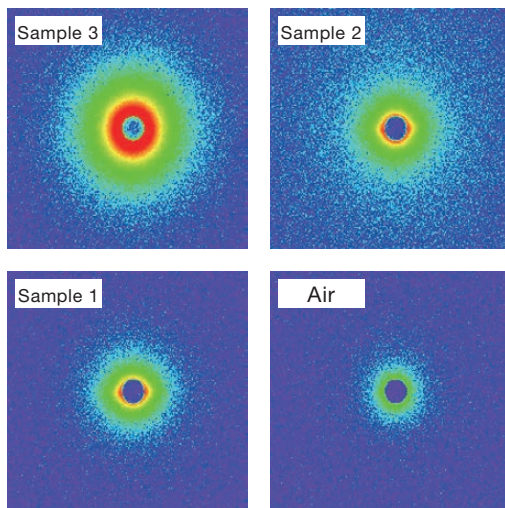


Figure 7 SAXS 2D images.

Figure 8 shows the  $I$ - $q$  profiles of the obtained scattering patterns made into one dimension. A clear difference was confirmed between the Sample 2 to which the organic additive had been added and the Sample 1 to which the organic additive had not been added in the region where the  $q$  is larger than about  $0.3 \text{ nm}^{-1}$ . This difference is considered to be due to the scattering by the nano inclusions generated by the organic additive. Also, since the inclination of the  $I$ - $q$  immediately changes to  $q^{-4}$  from the plateau region, the nano inclusions are considered to be spherical from checking the structure information shown in Figure 3. This is also consistent with the shape of the nano inclusions obtained from the TEM image.

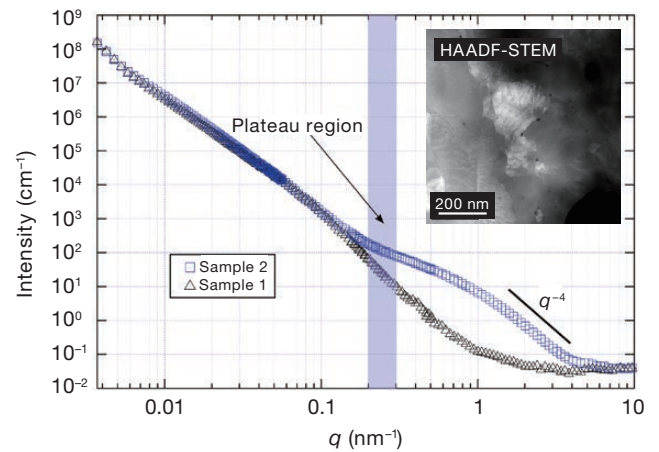


Figure 8 The  $I$ - $q$  profile of the Sample 2.

And the preliminary analysis using the Guinier plot estimated that the particle size of these nano inclusions to be about 5 to 6 nm.

However, since the scattering of the nano inclusions shows a gradual curve, and the nano inclusions as large as 10 nm are observed also in the TEM observation results, the nano inclusions are considered to have a wide particle size distribution. For this reason, the particle size estimated from the Guinier plot may be larger than the average particle size. Therefore, for detailed analysis, a curve fitting and so on taking the particle size distribution into consideration are necessary.

Next, Figure 9 shows the  $I$ - $q$  profiles of before and after annealing (Sample 2, Sample 3) with respect to the structural changes caused by the annealing. The level of the scattering intensity caused by the nano inclusions in the region where the  $q$  is larger than about  $0.3 \text{ nm}^{-1}$ , which had been confirmed before the annealing, decreased after the annealing. On the other hand, the scattering intensity increased in the region where the  $q$  is lower than about  $0.3 \text{ nm}^{-1}$ .

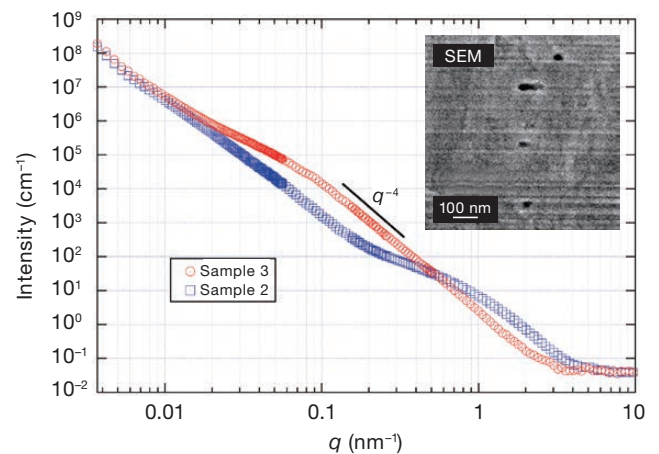


Figure 9 The  $I$ - $q$  profile of the Sample 3.

The Guinier range is shifted towards the Low- $q$  side in comparison with the Sample 2. Therefore, it is presumed that a structure of at least a hundred and tens of nm exists there. On the other hand, since the voids confirmed by the SEM observation are about several hundred nm, the origin of the scattering in the Low- $q$  is considered to be due to voids.

In order to further analyze, an  $I$ - $q$  profile only by the nano inclusions was created by subtracting the  $I$ - $q$  profile of the Sample 1, which is the scattering only from copper, from the  $I$ - $q$  profile of the Sample 2 and the Sample 3 containing the nano inclusions. Figures 10 (a) and (b) show the results. Then, with respect to these  $I$ - $q$  profiles, a fitting was performed by changing the radius  $R$  of the sphere using the equation (6). The result is shown in Figure 10). The average size of the inclusions increased from 5.0 nm, which was the value before the annealing, to 72.0 nm, which was the value after the annealing. The half width of the particle size distribution also increased (The insertion figure in Figure 10). That is, large inclusions which had not been confirmed before the annealing came to exist.

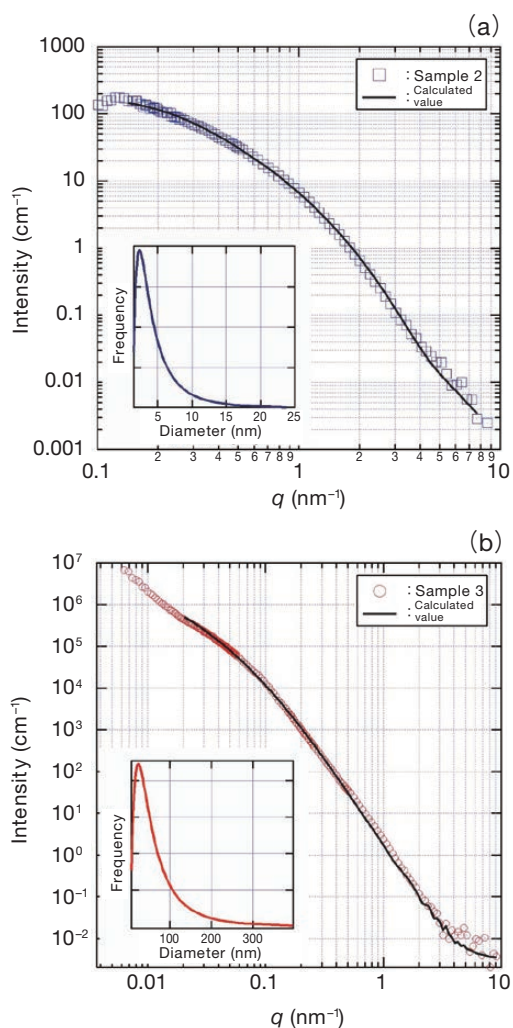


Figure 10 The curve-fitting of the  $I$ - $q$  profiles. (a) Sample 2, (b) Sample 3

Together with these results, the observation results by a TEM and a SEM, and the decrease in the yield strength after the annealing compared to before the annealing, the migration of the dislocations by the annealing and the accompanying inclusion movement to the grain boundary occurred, and it resulted in the aggregation and the disappearance which led to generate voids (Figure 11). On the other hand, small inclusions also remained, and they are presumed to be CuS which could not be captured by the TEM-EDX this time. Since the melting point of CuS is 500°C, it is considered that the possibility of vaporization is low at the annealing at 300°C.

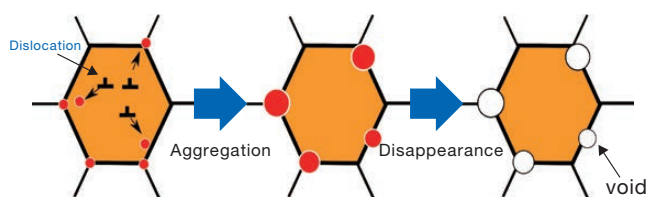


Figure 11 The Movement of the nano inclusions in the copper foil.

#### 4. CONCLUSION

In this study, the SAXS measurement was used to perform the bulk evaluation of the nano inclusions in the electrodeposited copper foil before and after the annealing.

With respect to the nano inclusions, it was found that the size was changed by the annealing.

Examining by taking the observation results with an electron microscope into account, it is considered that the nano inclusions which had been contained at the manufacturing of the film were dispersed in and out of the crystal, and bounced out to the crystal grain boundary together with the dislocations inside the crystal by annealing, and aggregated causing change in its size. These nano inclusions are considered to be CuS and organic structures containing at least carbon and sulfur, and those have low boiling points, then they had disappeared by the annealing at 300°C and the voids were formed.

In the future, we will clarify the correlation between the inclusions and the various physical properties, and we will develop technologies capable of freely easily deriving various properties.

#### ACKNOWLEDGEMENT

The tests using a synchrotron radiation used in this paper were performed by the Beamline BL19B2 with the approval of the Japan Synchrotron Radiation Research Institute (JASRI) as an Industry Creation Program.

(Theme number: No.2012B1896)

## REFERENCES

- 1) Ching An Huang, Jo Hsuan Chang, Fu-Yung Hsu, Chih Wei Chen, :  
“Electropolishing behaviour and microstructures of copper deposits electroplated in an acidic copper-sulphuric bath with different thiourea contents” *Surface and Coatings Technology*, Volume 238, 15 (2014), pp. 87-92.
- 2) Y.L. Kao, : “The annealing behavior of copper deposit electroplated in sulfuric acid bath with various concentrations of thiourea”, *Materials Science and Engineering A*, 382(2004), pp. 104-111.
- 3) F. Zhang, J. Ilavsky, G Long, J. Quintana, A. Allen, P. Jemian, :  
“Glassy Carbon as an Absolute Intensity Calibration Standard for Small-Angle Scattering”, *Metallurgical and Materials Transactions A*, Volume 41, Issue 5, pp. 1151–1158.
- 4) J. Ilavsky and P. Jemian, : “Irena: tool suite for modeling and analysis of small-angle scattering” *Journal of Applied Crystallography*, 42(2009), pp. 347–353.